



저작자표시-비영리-변경금지 2.0 대한민국

이용자는 아래의 조건을 따르는 경우에 한하여 자유롭게

- 이 저작물을 복제, 배포, 전송, 전시, 공연 및 방송할 수 있습니다.

다음과 같은 조건을 따라야 합니다:



저작자표시. 귀하는 원저작자를 표시하여야 합니다.



비영리. 귀하는 이 저작물을 영리 목적으로 이용할 수 없습니다.



변경금지. 귀하는 이 저작물을 개작, 변형 또는 가공할 수 없습니다.

- 귀하는, 이 저작물의 재이용이나 배포의 경우, 이 저작물에 적용된 이용허락조건을 명확하게 나타내어야 합니다.
- 저작권자로부터 별도의 허가를 받으면 이러한 조건들은 적용되지 않습니다.

저작권법에 따른 이용자의 권리는 위의 내용에 의하여 영향을 받지 않습니다.

이것은 [이용허락규약\(Legal Code\)](#)을 이해하기 쉽게 요약한 것입니다.

[Disclaimer](#)

의 학 박 사 학 위 논 문

대동맥판막 석회화의 비대칭 정도가
경피적 대동맥판막 치환술 후 판막주위
역류 및 추가 풍선확장의 성적에 미치는
영향

**Quantified Degree of Eccentricity of Aortic
Valve Calcification Predicts Risk of
Paravalvular Regurgitation and Response to
Balloon Post-Dilation after Self-Expandable
Transcatheter Aortic Valve Replacement**

2016년 8월

서울대학교 융합과학기술 대학원

분자의학 및 바이오제약 전공

박 준 빈

대동맥판막 석회화의 비대칭 정도가
경피적 대동맥판막 치환술 후 판막주위
역류 및 추가 풍선확장의 성적에 미치는
영향

지도교수 김 효 수

이 논문을 의학박사 학위논문으로 제출함

2016년 8월

서울대학교 융합과학기술 대학원

분자의학 및 바이오제약 전공

박 준 빈

**Quantified Degree of Eccentricity of Aortic
Valve Calcification Predicts Risk of
Paravalvular Regurgitation and Response to
Balloon Post-Dilation after Self-Expandable
Transcatheter Aortic Valve Replacement**

by Jun-Bean Park

A thesis submitted in partial fulfillment of the requirements for
the degree of Doctor of Philosophy in Medicine
(Molecular Medicine and Biopharmaceutical Sciences)
in Seoul National University, Seoul, Korea

August 2016

Abstract

Quantified Degree of Eccentricity of Aortic Valve Calcification Predicts Risk of Paravalvular Regurgitation and Response to Balloon Post-Dilation after Self-Expandable Transcatheter Aortic Valve Replacement

Jun-Bean Park

Department of Molecular Medicine and Biopharmaceutical Sciences

Graduate School of Convergence Science and Technology

Seoul National University

Objectives: We sought to investigate the prognostic value of aortic valve calcification (AVC) eccentricity in predicting the risk of paravalvular regurgitation (PVR) and the response to balloon post-dilation (BPD) in patients undergoing transcatheter aortic valve replacement (TAVR).

Background: Limited data exist regarding the impact of AVC eccentricity on the risk of significant PVR and the response to BPD.

Methods: We analyzed 85 patients with severe aortic stenosis who underwent self-expandable TAVR. AVC was quantified as the total amount of calcification (total AVC load) and as the eccentricity of calcification (AVC eccentricity index) using calcium volume scoring with contrast computed tomography angiography (CTA). The AVC eccentricity index was defined as the maximum absolute difference in calcium volume scores between 2 adjacent sectors, which was not confined to leaflet sectors. The perimeter undersizing index was calculated to take the

relative size of the device to the annulus into account. PVR was defined as present when blood flowed abnormally through a channel between the device and annulus as a result of incomplete sealing. The primary study endpoint was the occurrence of significant PVR, defined as \geq moderate PVR. The secondary endpoint was the response to BPD, a widely adopted strategy to reduce the degree of PVR in cases of frame under-expansion.

Results: Total load of and eccentricity index of AVC were significant predictors for the occurrence of \geq moderate PVR and AVC eccentricity index had a better predictive value than total AVC load (area under the curve = 0.863 versus 0.760, p for difference = 0.006). In multivariate analysis, AVC eccentricity index was an independent predictor for the risk of \geq moderate PVR regardless of perimeter undersizing index. There was no incidence of \geq moderate PVR in patients with extensive (total AVC load of $>1099.1 \text{ mm}^3$) but symmetric calcification (AVC eccentricity index of $\leq 272.8 \text{ mm}^3$). The AVC eccentricity index was the only significant parameter to predict the poor response to BPD (area under the curve = 0.775, p = 0.004). The addition of AVC eccentricity index to perimeter undersizing index significantly increased the discriminative ability of the prediction model and improved the classification of the risk estimation, whereas total AVC amount did not.

Conclusions: Pre-procedural assessment of AVC eccentricity using CTA provides useful predictive information on the risk of significant PVR and the response to BPD in patients undergoing TAVR with self-expandable valves.

Keywords: eccentric aortic valve calcification, transcatheter aortic valve replacement, paravalvular regurgitation, balloon post-dilation, computed tomography angiography

Student Number: 2013-30834

Contents

Abstract -----	i
Contents -----	iii
List of tables -----	iv
List of figures -----	v
List of abbreviations -----	vi
Introduction -----	1
Methods -----	2
Results -----	7
Discussion -----	22
References -----	31
국문초록 -----	35

List of tables

Table 1. Baseline Characteristics According to the Presence of More Than or Equal to Moderate PVR -----	8~10
Table 2. CTA Parameters According to the Presence of More Than or Equal to Moderate PVR -- -----	11~12
Table 3. Univariate Analysis for More Than or Equal to Moderate PVR and Successful Response to BPD -----	13
Table 4. Multivariate Analysis for More Than or Equal to Moderate PVR -----	15
Table 5. Incremental Predictive Values of Eccentricity of or Total Amount of AVC for Outcomes -----	16

List of figures

Figure 1. Quantification of Total Amount of and Eccentricity of AVC -----	5
Figure 2. Cut-off Values of Eccentricity of and Total Amount of AVC for Prediction of \geq Moderate PVR -----	17
Figure 3. Comparison between Eccentricity of and Total Amount of AVC with Regard to Occurrence of \geq Moderate PVR -----	18
Figure 4. Cut-off Values of Eccentricity of and Total Amount of AVC for Prediction of Response to BPD -----	19
Figure 5. Comparison between Eccentricity of and Total Amount of AVC with Regard to Response to BPD -----	20
Figure 6. Predictive Power of AVC Eccentricity Index in Comparison with Conventional Parameter Measured by Leaflet-based Method -----	21
Figure 7. Representative example of a patient with balanced calcification at 3 leaflets -----	24
Figure 8. Representative example of a patient with asymmetric calcification of a bicuspid aortic valve -----	25
Figure 9. Representative example of a patient with commissural calcification -----	26
Figure 10. Schematic Figure Illustrating Possible Mechanism for Impact of AVC Eccentricity on Response to BPD -----	29

List of abbreviations

AS = aortic stenosis

AUC = areas under the curves

AVC = aortic valve calcification

BPD = balloon post-dilation

CTA = computed tomography angiography

HU = Hounsfield units

IDI = integrated discrimination improvement

MCV = Medtronic CoreValve

NRI = net reclassification index

PVR = paravalvular regurgitation

ROC = receiver-operating characteristic

SAVR = surgical aortic valve replacement

TAVR = transcatheter aortic valve replacement

TEE = transesophageal echocardiography

Introduction

Transcatheter aortic valve replacement (TAVR) is increasingly accepted as a standard of care for inoperable patients with severe aortic stenosis (AS) (1), and as a comparable treatment option to surgical aortic valve replacement (SAVR) in AS patients with high operative risk (2). Given the favorable outcomes with clear advantage of being less invasiveness of this state-of-the-art technology, attempts are already in place to extend the indication of TAVR to AS patients with intermediate or low operative risk (3,4).

While mounting evidence is emerging to ensure the effectiveness of TAVR, concerns about safety issues have been consistently raised, especially regarding the risk of paravalvular regurgitation (PVR). The frequency of PVR after TAVR is substantially higher than that after SAVR (5), and, more importantly, PVR is associated with poor short-, mid-, and long-term prognosis (6-9). Thus, intense attention has been gained to identify reliable predictors for the risk of significant PVR, which can be used in guiding patient selection or in determining a tailored treatment strategy.

The severity and location of aortic valve calcification (AVC) measured by computed tomography angiography (CTA) have been reported as important contributing factors to the risk of PVR (10-12). However, the impact of the eccentricity of AVC on PVR risk is incompletely understood to date. Furthermore, because AVC eccentricity was evaluated visually in a qualitative manner (11,13), it is difficult to apply these study results to clinical practices. Hence, the aim of this study was to assess the predictive value of AVC eccentricity for the development of PVR following TAVR with Medtronic CoreValve (MCV) system. Additionally, we also sought to investigate whether AVC eccentricity can predict the response to balloon post-dilation (BPD), a useful tool to reduce the amount of PVR but potentially risky procedure that threaten to increase complication rates such as stroke.

Methods

Study population

From January 2011, we prospectively recruited patients with severe AS undergoing TAVR with the self-expandable MCV prosthesis (Medtronic, Minneapolis, MN, USA) at Seoul National University Hospital (Seoul, Republic of Korea), Asan Medical Center (Seoul, Republic of Korea), and National Heart Centre Singapore (Mistri Wing, Singapore). Eligibility for TAVR was established based on the consensus of the multidisciplinary team, including cardiologists, surgeons, and cardiac anesthesiologists, at each institute. Clinical data were carefully collected, including demographic characteristics, traditional risk factors for cardiovascular disease, and surgical risk scores. The protocol of this prospective study complied with the declaration of Helsinki, and was approved by the institutional review boards of each site. All patients gave written informed consent for enrollment.

Procedures

All patients underwent comprehensive evaluation before TAVR using a standardized protocol, including aortography, coronary angiography, echocardiography, and CTA. The details of the implantation technique have been previously described (14). All procedures were performed under general anesthesia and transesophageal echocardiography (TEE) guidance. Bilateral common femoral artery access was obtained with standard percutaneous access techniques and was closed with PerClose Proglide (Abbott Vascular) devices. The size of valve prosthesis was selected based on pre-enrollment aortic annulus measurements obtained by all available imaging modalities including CTA and TEE. The choice of whether to perform balloon pre-dilation was at the discretion of the operator depending on the individual risk and benefit of procedure. The prosthesis was deployed and implanted within aortic annulus over a stiff wire under rapid ventricular pacing. After valve deployments, the severity of PVR was evaluated by using an integrative approach (15). Briefly, PVR was defined as present when blood flowed in the direction opposite to that of physiologic blood flow through a channel between the device and annulus as a result of incomplete sealing. The angiographic degree of

paravalvular or transvalvular regurgitation was evaluated after approximately 10 minutes of bioprosthesis deployment to allow its maximum expansion, with the classification based on Seller's criteria (15-17). All echocardiographic imaging windows including short-axis view were used for the comprehensive evaluation of the location, number, and severity of PVR. The echocardiographic grading of PVR was based on the multiparametric and semi-quantitative assessment as recommended by current guidelines (17). Great care was taken to assess the proportion of PVR jet arc length to the short-axis view circumference of the valved stent. The PVR assessment was performed by an independent analyzer blinded to CTA results. BPD was considered as a therapeutic option in patients developing PVR after device deployment. Indications and techniques of BPD were left to the operator's discretion on the basis of the perceived proper placement of the prosthesis and the severity of PVR. Typically, BPD was performed in patients with significant PVR due to overt frame under-expansion or inadequate sealing, avoiding it in cases due to evident high or low deployment.

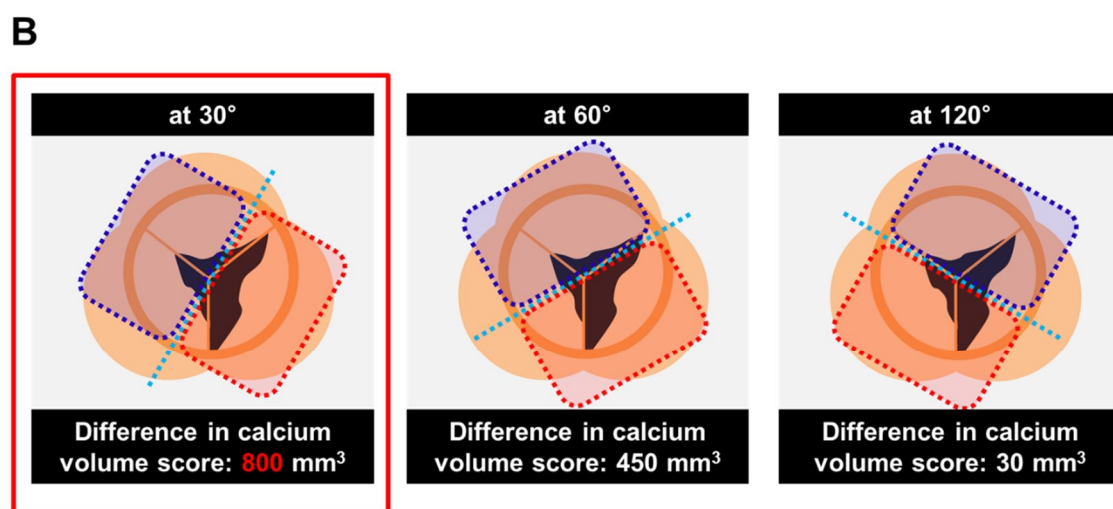
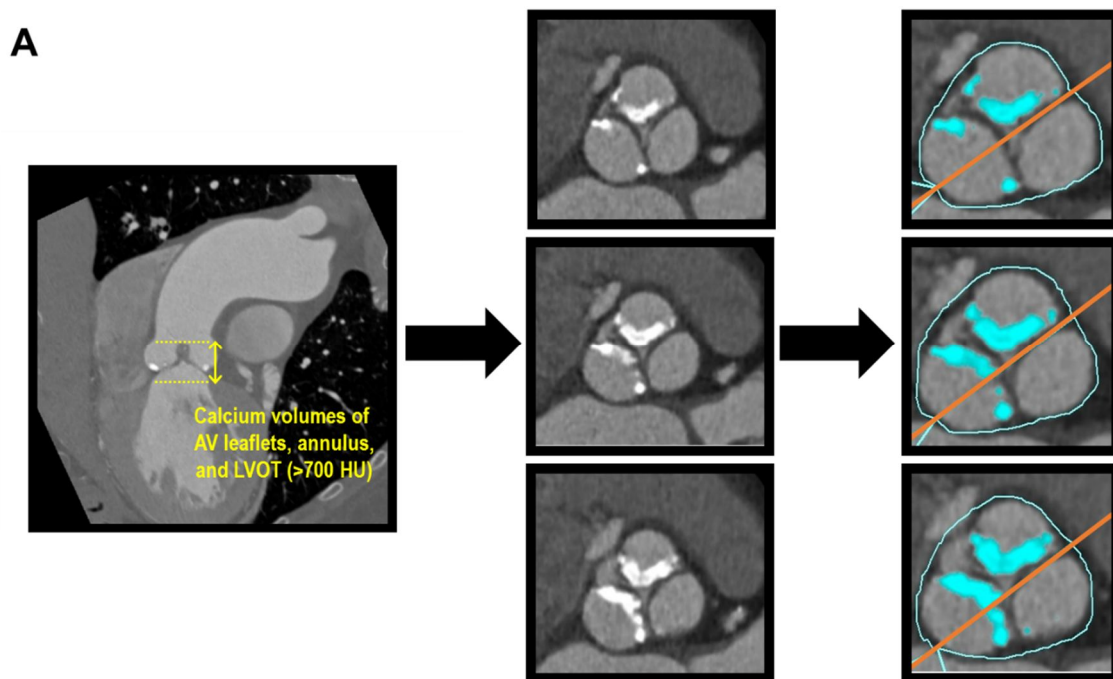
Aortic annular measurement by CTA

The aortic annulus size was comprehensively measured during mid-systole. The annular perimeter and area were measured by planimetry in the short-axis plane of the aortic root. The perimeter undersizing index was calculated using the formula: $([\text{nominal MCV perimeter} - \text{measured perimeter}] / \text{nominal MCV perimeter}) \times 100$. The area undersizing index was also calculated by the formula: $([\text{nominal MCV area} - \text{measured area}] / \text{nominal MCV area}) \times 100$.

CTA-based analysis of AVC

AVC was quantified using calcium volume scoring on pre-procedural contrast-enhanced CTA images with a CT software program (Rapidia 2.8; INFINITT, Seoul, Korea), as the reproducibility and potential of this method has been demonstrated in recent studies (11,18). Forty images of the short axis planes of aortic root with 1 mm slice thickness and zero gap were reconstructed. The region of interest for calcium volumes included the total leaflet region and left ventricular outflow tract region, which was defined as the cross-sectional area from the leaflet tips to the annulus and the area from the

annulus to 5 mm inferior to it, respectively. Calcium volumes were measured in these images and the total amount of (total AVC load) and the eccentricity of calcification (AVC eccentricity index) were quantified. Every voxel above the predefined threshold of 700 Hounsfield units (HU) was counted as calcification, with manual adjustment in those for whom the threshold was not appropriate. The threshold of 700 HU was selected based on the aorta lumen attenuation which is not over 700 in the most of the cases. All voxels exceeding the threshold were summed up in planes and through the planes to calculate total AVC load (Figure 1A). To assess AVC eccentricity index, we drew an imaginary “cutting line” that passed through the center of aortic valve cusps and divided the horizontal plane of aortic valve into 2 sectors (Figure 1A-B). Twelve sets of 2 sectors were generated by rotating the cutting line in 15 degree intervals, and the maximum absolute difference in calcium volume scores between 2 adjacent sectors was defined as AVC eccentricity index. For the sake of comparison, the asymmetry of AVC was also assessed by the conventional method based on the maximum difference in AVC between any 2 leaflet sectors, as previously described (11). All CTA data were analyzed by a single core laboratory (Seoul National University Hospital) in a blinded manner.



AVC eccentricity index
= Maximum difference among 24 images (every 15°)
= 800 mm³

Figure 1. Quantification of Total Amount of and Eccentricity of AVC

(A) Quantification of the total amount of AVC and the degree of AVC eccentricity.

(B) A schematic demonstration showing the assessment of AVC eccentricity. Twelve sets of 2 sectors within the AV were generated by drawing an imaginary “cutting line” that divides the AV into 2 sectors, and rotating this cutting line in 15 degree intervals. The maximum absolute difference in calcium volume scores between 2 adjacent sectors were defined as AVC eccentricity index.

AV = aortic valve; AVC = aortic valve calcification.

Definition of endpoints

The primary endpoint was the occurrence of significant PVR, defined as more than or equal to moderate PVR at the end of TAVR procedure. The secondary endpoint was the response to BPD, and it was considered effective if the severity of PVR was improved by at least 1 degree and the final PVR was graded as less than or equal to mild.

Statistical analysis

Continuous variables are given as mean \pm standard deviation or median (interquartile range), and categorical data as numbers (percentages), respectively. Continuous and categorical variables were compared by the Mann-Whitney U test and Fisher exact test, respectively. A univariate logistic regression analysis was used to select the potential predictors for the occurrence of \geq moderate PVR and the response to BPD. Univariate predictors with a p value <0.05 were entered into a multivariate logistic regression model to determine independent predictors. The results from the conventional maximum likelihood estimation of the logistic model were further corroborated by Firth's penalized likelihood logistic regression to reduce small-sample bias (19). Using the receiver-operating characteristic (ROC) curves, we calculated the sensitivities and specificities of cut-off values of total AVC load and AVC eccentricity index to determine the optimal value best predicting the risk of \geq moderate PVR and the poor response to BPD. The areas under the curves (AUC) were computed to assess the predictive ability of the variables of interest on the risk of significant PVR. To explore the incremental value of AVC eccentricity index and/or total AVC load in predicting endpoints, we constructed multiple models, starting with perimeter undersizing index alone. Then, AVC eccentricity index and/or total AVC load was added to generate sequential models. The AUC of each model was calculated and compared for significant difference. To further support the additive value of total AVC load and/or AVC eccentricity index to perimeter undersizing index, we also performed the category-free net reclassification index (NRI) and integrated discrimination improvement (IDI) analyses. All statistical analyses were conducted with SPSS version 22 (IBM SPSS Statistics, Chicago, IL) and R version 3.2.1 (www.r-project.org). A two-sided p value <0.05 was considered as significant.

Results

Baseline Characteristics

A total of 85 patients were included in the analysis. The clinical, echocardiographic, and procedural characteristics of study population are summarized in Table 1. All patients (age 77.2 ± 7.1 years, 50.6% female) had severe aortic stenosis (mean pressure gradient 59.5 ± 19.4 mmHg, aortic valve area 0.65 ± 0.18 cm²). Seventy-four (87.1%) patients presented post-procedural PVR, which was trace in 40 (47.1%), mild in 21 (24.7%), and moderate in 13 patients (15.3%). No patient had severe PVR. There was no significant difference in clinical characteristics between patients with \geq moderate PVR and $<$ moderate PVR (Table 1). Left ventricular ejection fraction was significantly lower in patients with \geq moderate PVR than those without ($p = 0.005$). Clinical characteristics by quartiles of AVC eccentricity index are provided in Table 2. Patients from the higher quartiles of AVC eccentricity index had lower rates of diabetes mellitus, hypertension, and coronary artery disease, whereas other clinical variables did not significantly differ among quartiles.

AVC and Other CTA Parameters

Table 3 shows that the values of total AVC load and AVC eccentricity index were significantly greater in patients with \geq moderate PVR than those without (1149.9 ± 610.9 versus 667.3 ± 507.0 mm³, $p = 0.004$; 537.6 ± 253.5 versus 235.9 ± 210.9 mm³, $p < 0.001$, respectively). The angle between the axes of the left ventricular outflow tract and aorta was numerically greater in patients with \geq moderate PVR, but the difference was not statistically significant. There was no difference in annulus size measurements by CTA, including diameter, perimeter, and area. However, the magnitude of undersizing was significantly greater in patients with \geq moderate PVR than those with $<$ PVR.

Table 1. Baseline Characteristics According to the Presence of More Than or Equal to Moderate PVR

	All (n = 85)	PVR <moderate (n = 72)	PVR ≥moderate (n = 13)	<i>p</i> value
Clinical variables				
Age, years	77.2 ± 7.1	77.7 ± 7.4	74.9 ± 4.3	0.091
Male / female	42 / 43	34 / 38	8 / 5	0.382
Weight, kg	57.5 ± 10.5	57.8 ± 11.0	55.8 ± 6.8	0.350
Height, cm	157.2 ± 9.4	157.2 ± 9.6	157.5 ± 8.6	0.802
Body surface area, cm ²	1.57 ± 0.17	1.57 ± 0.18	1.55 ± 0.3	0.651
Diabetes mellitus	24 (28.2)	23 (31.9)	1 (7.7)	0.098
Hypertension	63 (74.1)	54 (75.0)	9 (69.2)	0.734
Dyslipidemia	58 (68.2)	49 (68.1)	9 (69.2)	1.000
Smoker	8 (9.4)	5 (6.9)	3 (23.1)	0.100
Coronary artery disease	42 (49.4)	36 (50.0)	6 (46.2)	1.000
Previous PCI	31 (36.5)	27 (37.5)	4 (30.8)	0.761
Previous CABG	6 (7.1)	5 (6.9)	1 (7.7)	1.000
Cerebrovascular disease	5 (5.9)	4 (5.6)	1 (7.7)	0.573
Peripheral vascular disease	7 (8.2)	5 (6.9)	2 (15.4)	0.290

NYHA functional class III or IV	62 (72.9)	55 (76.4)	7 (53.8)	0.104
Logistic EuroSCORE, %	14.0 ± 11.9	14.8 ± 12.4	9.3 ± 7.9	0.114
(median, IQR)	(10.7, 5.0 – 20.8)	(11.1, 2.8 – 9.0)	(5.5, 4.1 – 16.5)	
STS score, %	7.0 ± 7.8	7.5 ± 8.3	3.9 ± 2.5	0.080
(median, IQR)	(4.4, 2.6 – 7.8)	(4.9, 2.8 – 9.0)	(3.5, 2.2 – 4.8)	
Echocardiographic data				
LVEF, %	56.6 ± 10.9	57.6 ± 10.6	51.4 ± 11.6	0.005
Mean AV pressure gradient, mmHg	59.5 ± 19.4	59.1 ± 18.9	61.5 ± 22.9	0.826
Annulus, mm	21.6 ± 2.2	21.5 ± 2.2	22.2 ± 2.1	0.192
Moderate or severe AR	10 (11.8)	8 (11.1)	2 (15.4)	0.646
Moderate or severe MR	7 (8.2)	7 (9.7)	0 (0.0)	0.588
Procedural data				
Prosthesis size, mm				0.020
23	1 (1.2)	1 (1.4)	0 (0.0)	
26	43 (50.6)	34 (47.2)	9 (69.2)	
29	33 (38.8)	32 (44.4)	1 (7.7)	
31	8 (9.4)	5 (6.9)	3 (23.1)	

Values given as mean ± standard deviation or number (percentage), unless otherwise indicated.

PVR = paravalvular regurgitation; PCI = percutaneous coronary intervention; CABG = coronary artery bypass graft; NYHA = New York Heart Association;
IQR = interquartile range; STS = the Society of Thoracic Surgeons; LVEF = left ventricular ejection fraction; AV = aortic valve; AR = aortic regurgitation;
MR = mitral regurgitation.

Table 2. Clinical Characteristics According to Quartiles of AVC Eccentricity Index

	Q1 (n = 21) <105.3 mm ³	Q2 (n = 21) 105.3 – 225.2 mm ³	Q3 (n = 22) 225.3 – 401.2 mm ³	Q4 (n = 21) >401.2 mm ³	<i>p</i> value
Age, years	78.9 ± 7.1	78.2 ± 7.4	76.0 ± 7.2	75.9 ± 6.5	0.431
Male / female	6 / 15	11 / 10	14 / 8	11 / 10	0.139
Weight, kg	55.3 ± 10.0	59.9 ± 12.0	58.4 ± 8.3	56.3 ± 11.4	0.477
Height, cm	154.8 ± 8.5	158.1 ± 10.5	157.9 ± 8.6	158.1 ± 10.1	0.489
Body surface area, cm ²	1.52 ± 0.15	1.60 ± 0.20	1.59 ± 0.15	1.56 ± 0.18	0.472
Diabetes mellitus	6 (28.6)	11 (52.4)	5 (22.7)	2 (9.5)	0.021
Hypertension	14 (66.7)	20 (95.2)	16 (72.7)	13 (61.9)	0.045
Dyslipidemia	15 (71.4)	17 (81.0)	15 (68.2)	11 (52.4)	0.280
Smoker	1 (4.8)	0 (0.0)	2 (9.1)	5 (23.8)	0.058
Coronary artery disease	15 (71.4)	12 (57.1)	9 (40.9)	6 (28.6)	0.031
Previous PCI	12 (57.1)	8 (38.1)	5 (22.7)	6 (28.6)	0.108
Previous CABG	2 (9.5)	2 (9.5)	0 (0.0)	2 (9.5)	0.523
Cerebrovascular disease	1 (4.8)	2 (9.5)	2 (9.1)	0 (0.0)	0.748
Peripheral vascular disease	3 (14.3)	1 (4.8)	1 (4.5)	2 (9.5)	0.660

NYHA functional class III or IV	17 (81.0)	16 (76.2)	11 (50.0)	18 (85.7)	0.055
Logistic EuroSCORE, %	18.0 ± 12.8	12.1 ± 11.7	11.8 ± 13.5	14.0 ± 9.1	0.126
(median, IQR)	(16.9, 7.7 – 26.2)	(8.0, 4.2 – 15.0)	(8.2, 3.1 – 14.8)	(11.0, 5.8 – 22.7)	
STS score, %	7.3 ± 8.6	7.7 ± 7.5	6.9 ± 7.4	5.8 ± 7.9	0.782
(median, IQR)	(5.8, 3.0 – 7.3)	(4.8, 2.2 – 12.8)	(3.8, 2.4 – 9.7)	(3.9, 2.6 – 5.6)	

Values given as mean ± standard deviation or number (percentage), unless otherwise indicated.

Abbreviations as in Table 1.

Table 3. CTA Parameters According to the Presence of More Than or Equal to Moderate PVR

	All (n = 85)	PVR <moderate (n = 72)	PVR ≥moderate (n = 13)	<i>p</i> value
Annulus size				
Diameter, mm	25.4 ± 3.1	25.1 ± 3.0	26.9 ± 3.4	0.074
Perimeter, mm	75.1 ± 10.2	74.3 ± 9.9	79.9 ± 11.0	0.107
Area, mm ²	467.5 ± 117.0	456.0 ± 110.1	527.6 ± 137.4	0.102
Perimeter undersizing index, %	4.8 ± 9.6	6.2 ± 9.4	-2.9 ± 6.1	0.001
Area undersizing index, %	6.3 ± 16.9	8.5 ± 16.0	-7.1 ± 16.8	0.006
Calcification				
Total AVC load, mm ³	741.1 ± 548.7	667.3 ± 507.0	1149.9 ± 610.9	0.004
AVC eccentricity index, mm ³	282.0 ± 242.3	235.9 ± 210.9	537.6 ± 253.5	<0.001
∠ LVOT-Aorta, degree	20.9 ± 9.4	20.4 ± 9.7	23.3 ± 7.7	0.386

Values given as mean ± standard deviation or number (percentage), unless otherwise indicated.

AVC = aortic valve calcification; ∠ LVOT-Aorta = the angle between the axes of the left ventricular outflow tract and aorta; other abbreviations as in Table 2.

Predictors for significant PVR

As shown in Table 4, univariate analyses demonstrated that perimeter undersizing index, total AVC load, and AVC eccentricity index were significantly associated with the development of \geq moderate PVR, whereas neither clinical nor echocardiographic variables were predictive of its occurrence. In multivariable analyses, AVC eccentricity index and perimeter undersizing index, but not total AVC load, were independent predictors for the risk of \geq moderate PVR (Table 5). These results were unchanged when the multivariate analysis was repeated using Firth's penalized likelihood method. When the ROC curve analysis was performed in relation to AVC eccentricity index, the sensitivity and specificity for predicting \geq moderate PVR was 92.3% and 70.8%, respectively, with AVC eccentricity index of 272.8 mm³ as the best cut-off (AUC = 0.860, $p < 0.001$) (Figure 2A-B). Total AVC load was also a significant predictor for \geq moderate PVR (AUC = 0.755, $p < 0.001$) (Figure 2C-D), but its predictive power was significantly lower than that of AVC eccentricity index (p for difference in AUC = 0.006). Nine patients with total AVC load of >757.8 mm³ had AVC eccentricity index of ≤ 272.8 mm³, and these patients did not develop \geq moderate PVR after TAVR (Figure 3).

Table 4. Univariate Analysis for More Than or Equal to Moderate PVR and Effective Response to BPD

	≥moderate PVR			Effective BPD		
	OR	95% CI	<i>p</i> value	OR	95% CI	<i>p</i> value
AVC eccentricity index, per 100 mm ³ greater	1.555	1.207–2.005	0.001	0.558	0.347 – 0.897	0.016
Total AVC load, per 100 mm ³ greater	1.146	1.035–1.269	0.009	0.904	0.777 – 1.050	0.187
Perimeter undersizing index	0.885	0.815 – 0.960	0.003	1.083	0.985 – 1.191	0.098
∠ LVOT-Aorta, per 10 degree greater	1.034	0.969 – 1.105	0.313	1.019	0.932 – 1.113	0.683
Age, per year	0.946	0.868 – 1.030	0.202	1.045	0.954 – 1.146	0.345
Gender	0.559	0.167 – 1.874	0.346	0.900	0.217 – 3.726	0.884
Hypertension	0.750	0.206 – 2.733	0.663	3.333	0.605 – 18.371	0.167
Diabetes mellitus	0.178	0.022 – 1.449	0.107	3.846	0.684 – 21.642	0.126
Smoker	4.020	0.830 – 19.479	0.084	0.500	0.028 – 8.772	0.635
Logistic EuroSCORE	0.946	0.881 – 1.016	0.131	1.043	0.966 – 1.126	0.279
STS score	0.838	0.671 – 1.048	0.121	0.999	0.936 – 1.066	0.966
LVEF	0.957	0.913 – 1.004	0.069	0.984	0.905 – 1.070	0.710

OR = odds ratio; CI = confidential interval; other abbreviations as in Table 1, 2, and 3.

Table 5. Multivariate Analysis for More Than or Equal to Moderate PVR

	Classical maximum likelihood method			Firth's penalized likelihood method		
	OR	95% CI	<i>p</i> value	OR	95% CI	<i>p</i> value
AVC eccentricity index, per 100 mm ³ greater	1.793	1.041 – 3.091	0.035	1.633	1.055 – 2.9291	0.026
Total AVC load, per 100 mm ³ greater	0.891	0.712 – 1.116	0.316	0.9154	0.727 – 1.109	0.386
Perimeter undersizing index	0.904	0.821 – 0.994	0.037	0.915	0.828 – 0.994	0.034

Abbreviations are as in Table 1, 2, 3, and 4.

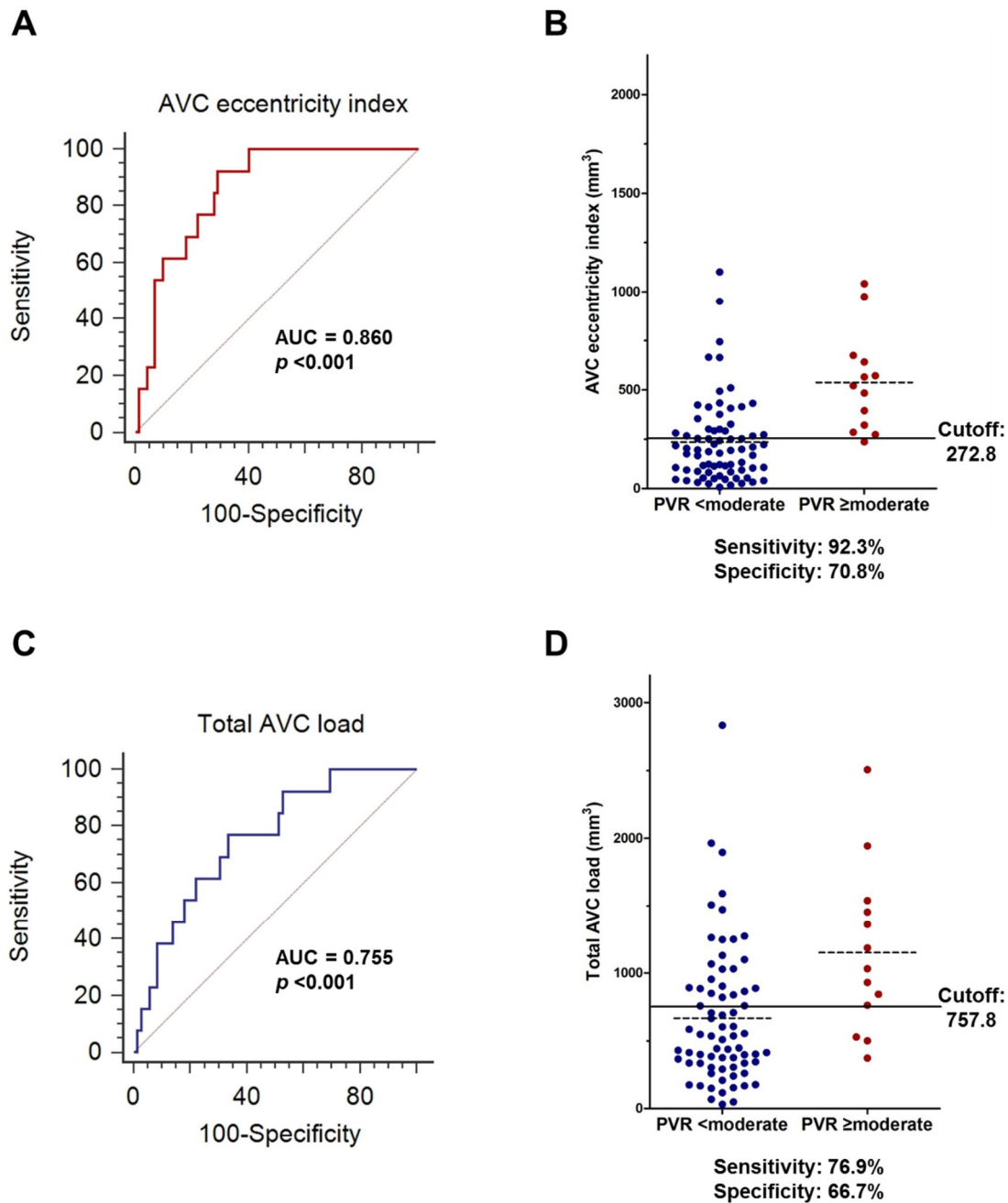


Figure 2. Cut-off Values of Eccentricity of and Total Amount of AVC for Prediction of \geq Moderate PVR

Using ROC curves, AVC eccentricity index (A) and total AVC load (C) can predict the occurrence of \geq moderate PVR after TAVR.

A dot plot showing patients with and without \geq moderate PVR according to the value of AVC eccentricity index (B) and total AVC load (D)

AUC = areas under the curves; PVR = paravalvular regurgitation.

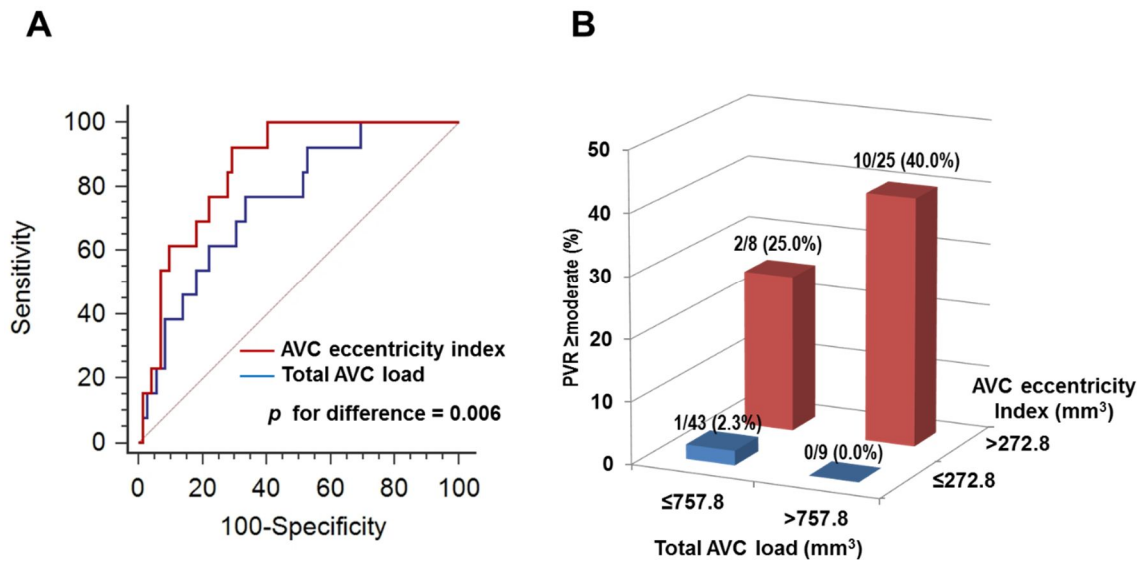


Figure 3. Comparison between Eccentricity of and Total Amount of AVC with Regard to Occurrence of \geq Moderate PVR

(A) The predictive value of AVC eccentricity index was greater than that of total AVC load for the risk of \geq moderate PVR.

(B) Incidence of \geq moderate PVR according to the total amount and eccentricity of AVC.

Abbreviations as in Figure 1 and 2.

Predictors for response to BPD

The BPD was performed in 35 patients and was effective in 23 patients (65.7%). Table 4 shows that a greater AVC eccentricity index was significantly associated with a lower probability of effective BPD. Neither total AVC load nor perimeter undersizing index was a significant determinant for the response to BPD, and AVC eccentricity index was the only significant predictor for the response to BPD. In ROC curve analysis, AVC eccentricity index had a significant predictive value for the response to BPD (AUC = 0.775, p = 0.004) (Figure 4A-B), but total AVC load did not (AUC = 0.623, p = 0.250) (Figure 4C-D). Compared with total AVC load, AVC eccentricity index provided significantly better discrimination ability in predicting the response to BPD (p for difference in AUC = 0.029). Notably, BPD was effective in patients with extensive (total AVC load $>1099.1 \text{ mm}^3$) but symmetric calcification (AVC eccentricity index of $\leq 272.8 \text{ mm}^3$) (Figure 5).

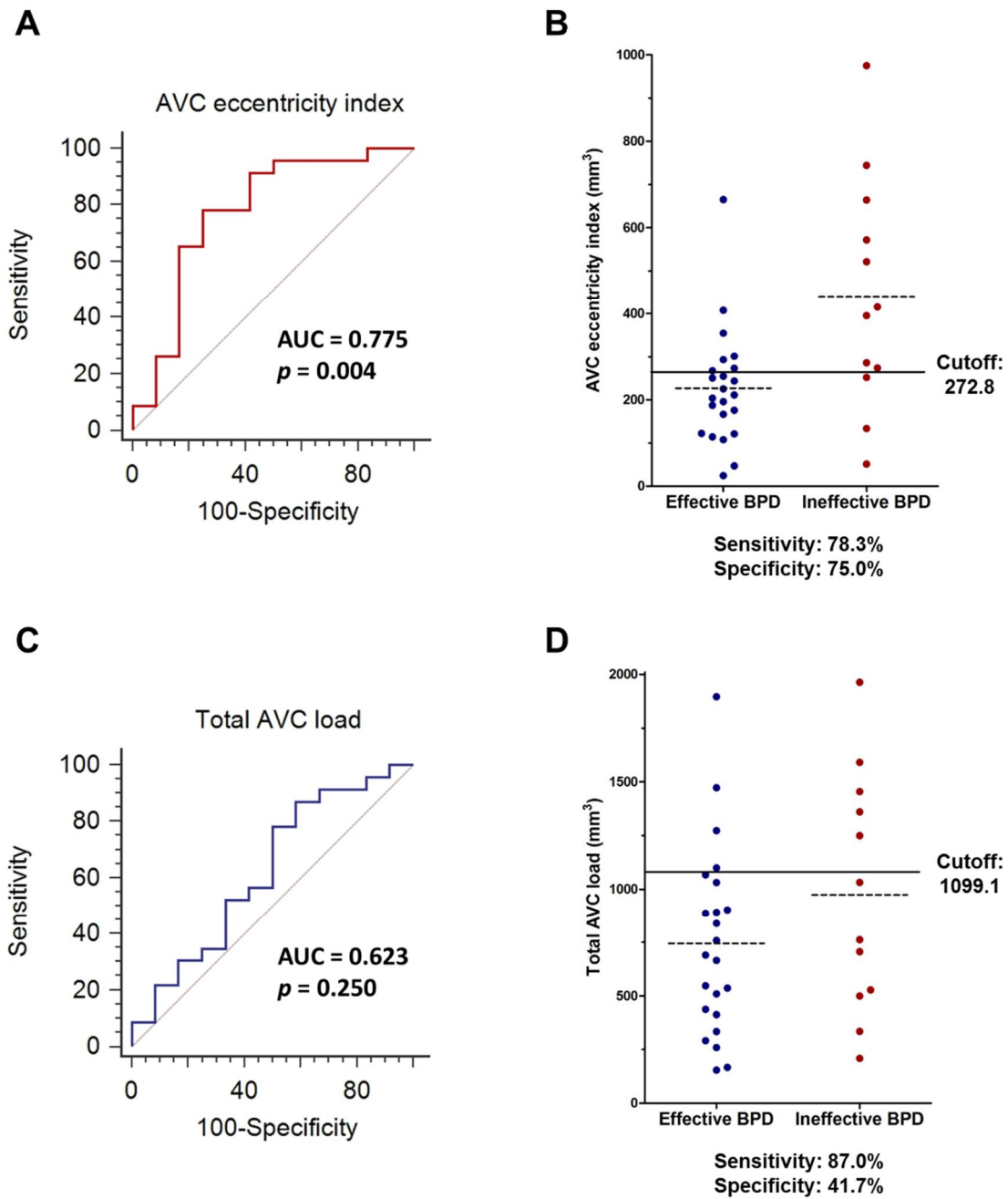


Figure 4. Cut-off Values of Eccentricity of and Total Amount of AVC for Prediction of Response to BPD

Using ROC curves, AVC eccentricity index (A) and total AVC load (C) can predict the effective response to BPD.

A dot plot showing patients with effective and ineffective BPD according to the value of AVC eccentricity index (B) and total AVC load (D)

BPD = balloon post-dilation; other abbreviations as in Figure 1, 2, and 3.

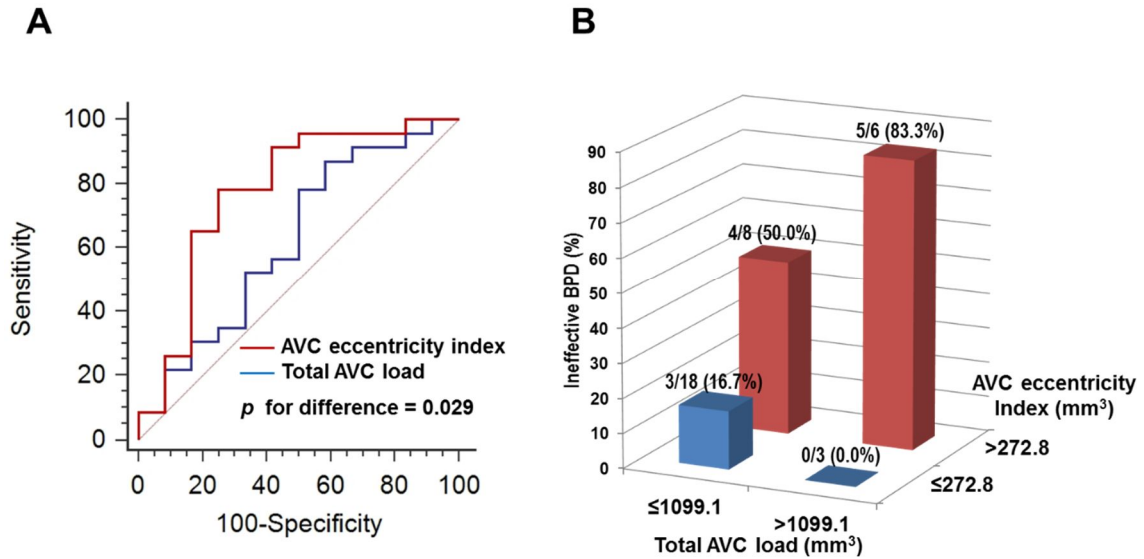


Figure 5. Comparison between Eccentricity of and Total Amount of AVC with Regard to Response to BPD

(A) The predictive value of AVC eccentricity index was greater than that of total AVC load for the response to BPD.

(B) Incidence of ineffective BPD according to the total amount and eccentricity of AVC.

Abbreviations as in Figure 1, 2, 3, and 4.

Predictive ability of AVC asymmetry determined by conventional method

When the eccentricity of AVC was assessed by the conventional method based on the maximum difference in AVC between 2 leaflet sector, it did not predict the occurrence of \geq moderate PVR (AUC = 0.602, $p = 0.258$) and the response to BPD (AUC = 0.551, $p = 0.632$) as accurately as AVC eccentricity index (Figure 6).

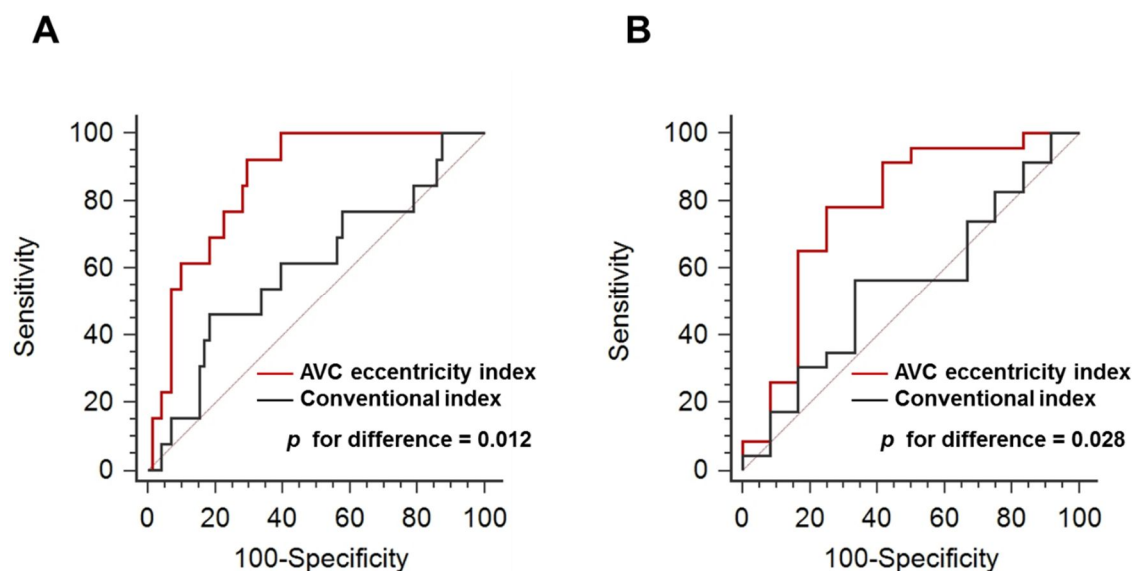


Figure 6. Predictive Power of AVC Eccentricity Index in Comparison with Conventional Parameter Measured by Leaflet-based Method

As compared with AVC eccentricity index, the conventional parameter of AVC asymmetry, as calculated from the maximum absolute difference in calcium volume scores between any 2 leaflets, did not predict the occurrence of \geq moderate PVR (A) and the response to BPD (B).

Abbreviations as in Figure 1, 2, 3, and 4.

Additional predictive value of AVC for endpoints

The addition of AVC eccentricity index significantly increased the predictive value of the model including perimeter undersizing index alone, but total AVC load did not (Table 5). The incorporation of both AVC eccentricity index and total AVC load further improved the predictive ability of the model for the risk of \geq moderate PVR and the response to BPD.

Discussion

The major findings of this study are summarized as follows; 1) the eccentricity of AVC quantified by CTA was an independent predictor for the occurrence of \geq moderate PVR immediately after TAVR with self-expandable valves, 2) the quantified degree of AVC eccentricity was a significant determinant for the response to BPD, and 3) the AVC eccentricity had a better predictive value than total amount of AVC for the risk of significant PVR and the response to BPD.

AVC and PVR

Given the higher incidence of PVR after TAVR than that developed after SAVR as well as its association with increased mortality even in mild degree (5-9,20), every effort should be made to prevent PVR. Furthermore, considering that attempts are already in place to extend the indication of TAVR to intermediate- and low-risk patients (3,4), evaluating the safety of TAVR, including PVR risk, should be of highest priority. In this regard, researchers have sought to identify markers to predict the risk of PVR, which can ultimately allow for improved patient selection and individualized pre-procedural strategic planning. Among various clinical, imaging, and procedural variables, several studies have emphasized the importance of assessing AVC for the prediction of PVR risk (10-13,21,22). In particular, previous studies showed that the total amount of and location of AVC predict the risk of PVR (11-13).

However, there has been few data available on whether AVC eccentricity can be a useful predictor for the development of significant PVR. Our study demonstrated that AVC eccentricity index quantified by CTA had a better predictive value for \geq moderate PVR risk as compared with total AVC load (Figure 3). Contrary to the expectations, a previous study using a semi-quantitative 4-grade scoring system revealed that the asymmetric calcification of the aortic valve cusps did not increase the post-procedural degree of PAR (13). Another study using calcium volume scores also showed that the asymmetry of AVC for leaflet sectors could not predict the occurrence of \geq mild PVR, whereas that of all other regions, such as annulus or left ventricular outflow tract, had significant predictive power for

the risk of PVR. (11). These findings can be explained by the fact that the asymmetry of AVC was assessed using the maximum absolute difference in AVC between any 2 leaflet sectors in the previous studies, which was different from our method to assess AVC.

Although the leaflet-based assessment of AVC eccentricity might be a more intuitive, our method of using the bisecting lines has clear advantages. First, the leaflet-based method can underestimate the eccentricity of AVC in patients with balanced calcification at 2 or more leaflets, for whom our method can more effectively demonstrate the eccentricity (Figure 7). Second, using leaflet-based method may lead to erroneous estimation of AVC eccentricity in patients with bicuspid aortic valve, particularly if the amount of calcification in each leaflet was similar (Figure 8). Third, because commissure could not be attributed to a particular leaflet sector, the maximum difference in AVC between 2 leaflet sectors might not reflect the true difference in AVC distribution in patients with significant commissural calcification (Figure 9). Finally, it is sometimes technically difficult to delineate different leaflets within the diseased aortic valve complex. Of note, when we repeated analyses using the maximum difference in AVC between 2 leaflet sectors as described in the previous study (11), this parameter did not significantly predict the occurrence of \geq moderate PVR and the response to BPD (Figure 6).

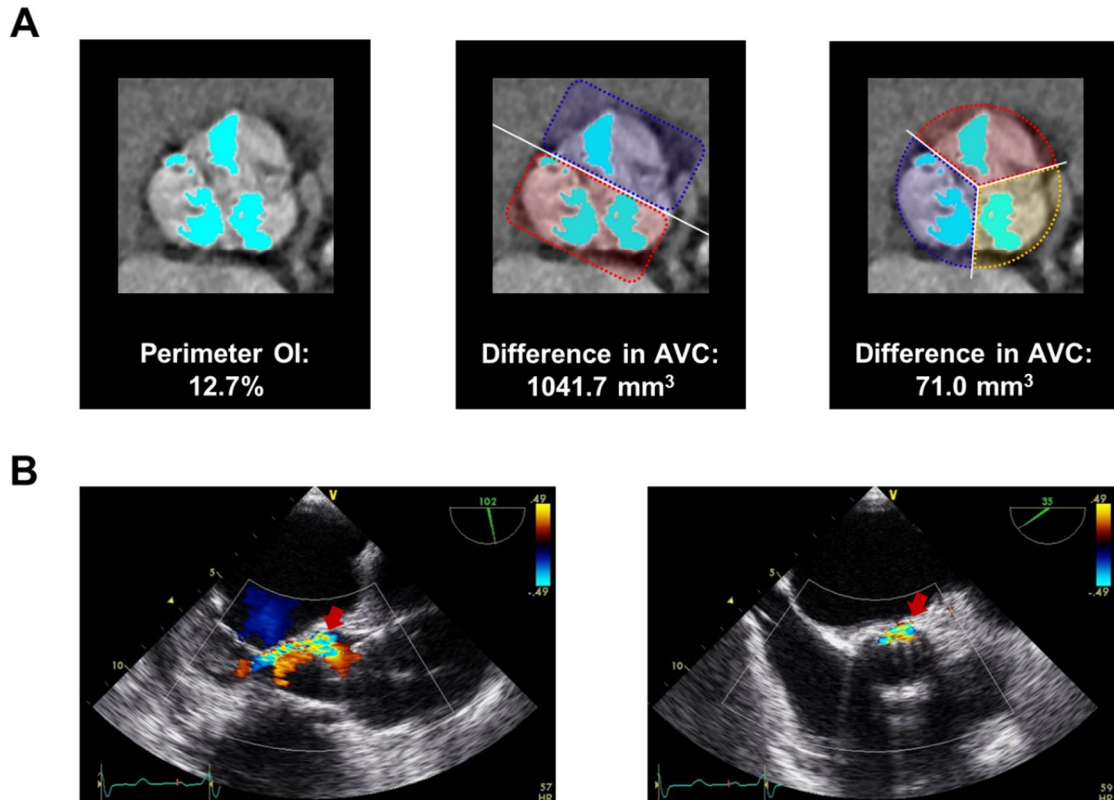


Figure 7. Representative example of a patient with balanced calcification at 3 leaflets

(A) CTA demonstrated calcification evenly distributed among right, left, and non-coronary leaflets (left panel). The implanted valve was oversized relative to the annular perimeter measured by CTA. The maximum difference in calcification was greater when assessed using a line bisecting the aortic valve (central panel) than using a line separating each leaflet (right panel).

(B) Two-dimensional TEE color Doppler imaging showed that this patient developed moderate PVR after the TAVR procedure (left and right panels).

UI = undersizing index.

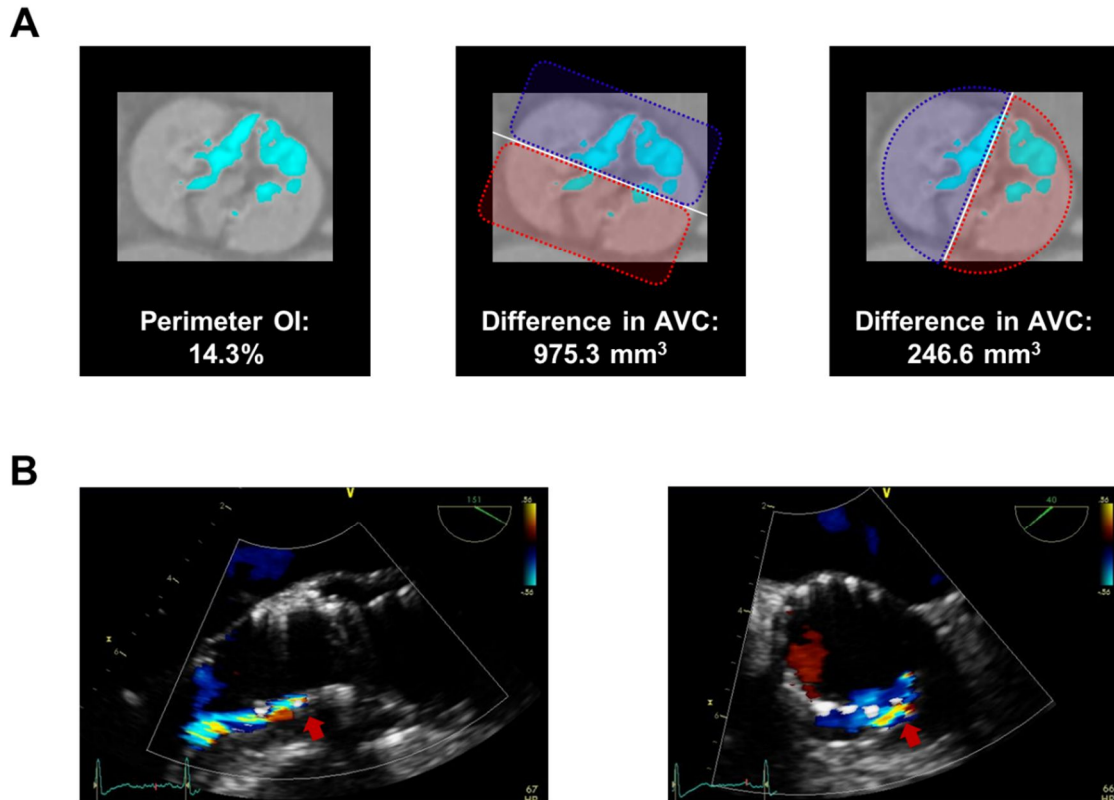


Figure 8. Representative example of a patient with asymmetric calcification of a bicuspid aortic valve

(A) CTA depicts elongated calcification along the edge of left and non-coronary leaflets (left panel). This patient received a prosthesis that was oversized in comparison with the CTA annular perimeter. The maximum difference in calcification was smaller as measured by the method using the bisecting lines (central panel) than using the leaflet-based method (right panel).

(B) In this patient, only trivial PVR was noted after the TAVR procedure (left and right panels). Abbreviations as in Figure 7.

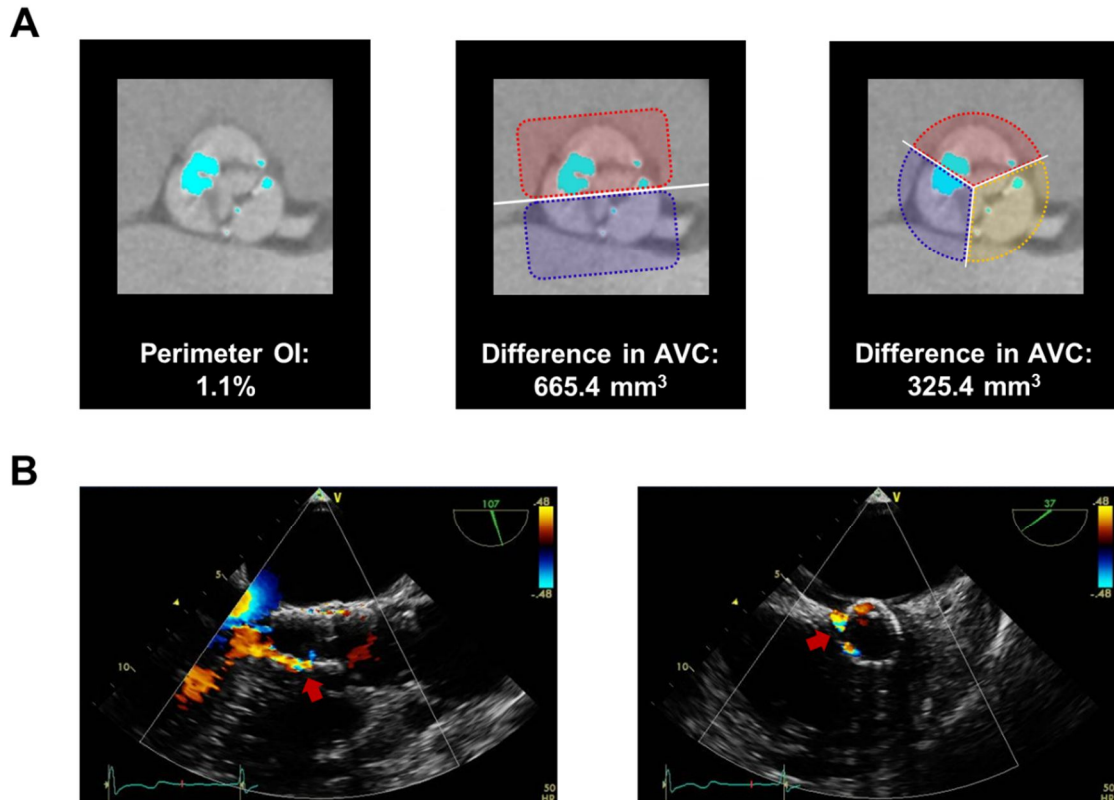


Figure 9. Representative example of a patient with commissural calcification

(A) CTA showed the presence of commissural calcification between right and non-coronary leaflets (left panel). The device size was nearly equal to the annular size in this case. When a line bisecting the aortic valve was used, the maximum difference in calcification was marked (central panel), whereas it was less pronounced when assessed using a line separating each leaflet (right panel).

(B) In this patient, PVR was considered moderate after valve deployment (left panel), and this was unchanged after BPD (right panel).

Abbreviations as in Figure 7 and 8.

AVC and device sizing

Previous studies suggested that a certain degree of prosthesis oversizing, usually 5% to 30%, is required to ensure its adequate adaptation to the aortic annulus and thus to prevent significant PVR. However, when aortic annulus measurements are in the overlapping area between 2 different prosthesis sizes, attention must be paid to the severity of calcification of the leaflets to minimize the potential risk of aortic root rupture (23). Specifically, the valve size could be nearly equal to the annular size in cases with severe calcification, whereas it should be at least ≥ 1 mm greater than the

annular size in cases without calcification. Furthermore, one study using balloon-expandable device showed that the strategy of intentionally under-expansion with additional BPD could reduce the risk of annular injury without increasing the risk of significant PVR (24). In this context, it is not surprising that the proportion of undersizing was recently reported to be as high as 30% and 45% in current and new-generation TAVR devices, respectively (25). Based on this evidence, we used the smaller of the 2 potential prosthesis choices, if the measurements of annulus size were on the borderline and the visually estimated extent of calcification was considered severe. This is one likely explanation why the degree of undersizing was significantly greater in patients with \geq moderate PVR, in whom the amount of calcification was significantly larger. Importantly, even when taking relative size of the device to annulus (i.e., perimeter undersizing index) into consideration, AVC eccentricity index was an independent predictor for the risk of \geq moderate PVR but total AVC load was not.

AVC and BPD

BPD has been proposed as a useful option to reduce the degree of PVR after TAVR. However, there have been concerns on potential risk of BPD, including stroke, conduction disturbance, or structural deterioration of the device (8,26,27). Indeed, in our study, although statistically insignificant probably due to a small sample size, patients undergoing BPD tended to have a higher incidence of stroke (2.9% [1/35] versus 2.0% [1/50], $p = 1.000$) or permanent pacemaker implantation (14.3% [5/35] versus 8.0% [4/50], $p = 0.478$) at 30 days after procedure, compared with those not undergoing BPD. In addition to the safety issue associated with BPD, its efficacy should be considered before performing the procedure. Previous studies suggested that BPD has no intended effect in reducing PVR in some patients (26-28). Indeed, the success rate of BPD was 54% and 63% in patients undergoing TAVI with balloon-expandable and self-expandable valves, respectively (26,28). Considering both the substantial proportion of non-responsive patients to BPD and the aforementioned BPD-related potential complications, more strict indications for this bailout procedure in selected cases can improve outcomes while minimizing adverse events. For this purpose, many efforts have been made aiming to identify useful parameters which can distinguish patients with a higher probability of favorable

outcomes from those without. One study with the balloon-expandable valves has reported that the total amount of AVC indicates the poor response to BPD (26). Although heavy AVC may result in an incomplete sealing of the paravalvular space regardless of prosthesis type, there has been no study to ascertain whether the degree of AVC can predict the procedural outcome of BPD in patients treated with self-expandable valve. Moreover, the usefulness of AVC eccentricity has never been evaluated as a parameter determining the response to BPD.

Our study firstly demonstrated that the degree of AVC eccentricity was a better determinant of the poor response to BPD than total amount of AVC. Given that the location of PVR corresponds to that of AVC (11,21), the eccentric AVC may hamper the uniform expansion of the balloon resulting in no further sealing of paravalvular space, particularly the location causing the PVR (Figure 10). In this regards, the risk of poor response to BPD might be higher in patients with eccentric AVC than in those with concentric AVC, if the degree of total AVC is similar.

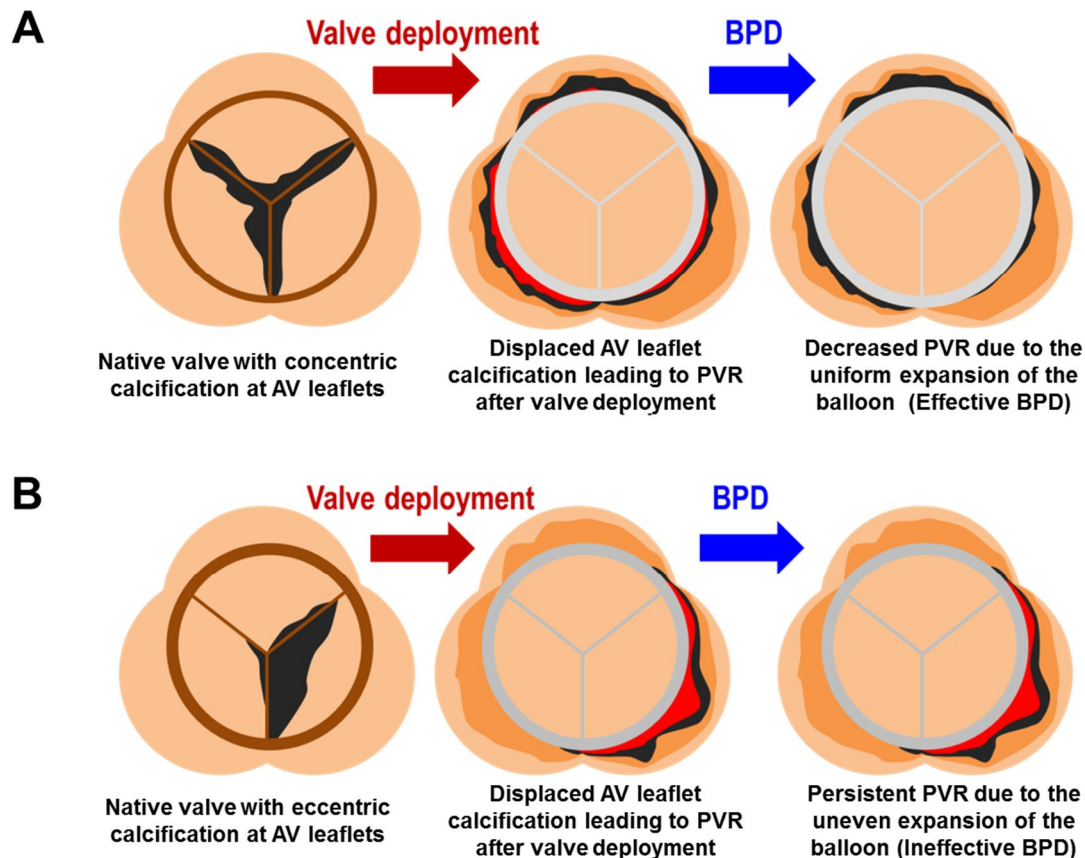


Figure 10. Schematic Figure Illustrating Possible Mechanism for Impact of AVC Eccentricity on Response to BPD

In a patient with concentric AVC, circumferential uniform expansion of the balloon can be achieved, which may seal the paravalvular space and thereby reduce the severity of PVR (A). However, the efficacy of BPD may be decreased in a patient with eccentric AVC, because it can hamper the uniform expansion of the balloon and thus further sealing of the paravalvular space (B).

Abbreviations as in Figure 1, 2, 3, and 4.

Study Limitations

First, as our sample size and event number were small, multivariate analyses were limited. To minimize potential statistical problems encountered with a small sample size in multivariate analyses, we employed the Firth's penalized likelihood method (19), by which the results were essentially unchanged. However, further studies with a large number of patients are needed to validate whether the degree of AVC eccentricity can be used to predict the risk of significant PVR and the response to BPD, and ultimately improve the outcomes in AS patients undergoing TAVR. Second, because the

present study was performed only on patients undergoing TAVR with self-expandable valves, our findings are not necessarily applicable to those treated with other types of device, including not only balloon-expandable valves but also new-generation valves. In particular, new-generation TAVR devices incorporate several features intended to minimize the risk of PVR, which may resolve the issue of PVR *per se* (29). Therefore, our hypothesis of the role of AVC in PVR prediction should be tested in patients receiving other valve types, although the CoreValve system is currently one of the most commonly used TAVR bioprosthesis and will continue to be used due to the advantages of being easy to perform and requiring less time. However, given that the indication of TAVR may expand to lower-risk AS patients in the future, the risk of PVR should be further minimized to justify TAVR rather than conventional surgery, which is a standard treatment for this population. Furthermore, the amount and eccentricity of AVC can also be of importance for the durability of all types of bioprosthetic valves. Indeed, due to cusp and commissural calcification, bioprosthetic valves used in SAVR undergo progressive structural deterioration which can affect their durability and result in functional failure requiring reoperation. Given that the less invasive nature of TAVR precludes the removal of calcified native aortic valve, the impact of AVC on the durability of devices can be a more significant problem after TAVR than SAVR. Finally, we used 700 HU as the cut-off point for the assessment of AVC on contrast CTA, however, such value has not been fully established and it is too high to usual threshold for calcium scoring which is 130 HU. We used contrast-enhanced CTA for the evaluation of calcium and try to reveal the meaning of AVC eccentricity. To mitigate this problem, we meticulously verify the presence of calcification and appropriately adjust the HU threshold of calcific regions.

Conclusion

Pre-procedural assessment of AVC eccentricity using CTA could provide useful predictive information on the risk of PVR and the efficacy of BPD in patients undergoing TAVR with self-expandable valves. This finding suggests that accurate measurement of AVC eccentricity might be helpful in patient selection and procedure planning in AS patients considered for TAVR.

References

1. Leon MB, Smith CR, Mack M et al. Transcatheter aortic-valve implantation for aortic stenosis in patients who cannot undergo surgery. *The New England journal of medicine* 2010;363:1597-607.
2. Smith CR, Leon MB, Mack MJ et al. Transcatheter versus surgical aortic-valve replacement in high-risk patients. *The New England journal of medicine* 2011;364:2187-98.
3. Wenaweser P, Stortecky S, Schwander S et al. Clinical outcomes of patients with estimated low or intermediate surgical risk undergoing transcatheter aortic valve implantation. *European heart journal* 2013;34:1894-905.
4. Piazza N, Kalesan B, van Mieghem N et al. A 3-center comparison of 1-year mortality outcomes between transcatheter aortic valve implantation and surgical aortic valve replacement on the basis of propensity score matching among intermediate-risk surgical patients. *JACC Cardiovascular interventions* 2013;6:443-51.
5. Genereux P, Head SJ, Hahn R et al. Paravalvular leak after transcatheter aortic valve replacement: the new Achilles' heel? A comprehensive review of the literature. *Journal of the American College of Cardiology* 2013;61:1125-36.
6. Kodali SK, Williams MR, Smith CR et al. Two-year outcomes after transcatheter or surgical aortic-valve replacement. *The New England journal of medicine* 2012;366:1686-95.
7. Gilard M, Eltchaninoff H, Iung B et al. Registry of transcatheter aortic-valve implantation in high-risk patients. *The New England journal of medicine* 2012;366:1705-15.
8. Unbehaun A, Pasic M, Dreyses S et al. Transapical aortic valve implantation: incidence and predictors of paravalvular leakage and transvalvular regurgitation in a series of 358 patients. *Journal of the American College of Cardiology* 2012;59:211-21.
9. Moat NE, Ludman P, de Belder MA et al. Long-term outcomes after transcatheter aortic valve implantation in high-risk patients with severe aortic stenosis: the U.K. TAVI (United Kingdom Transcatheter Aortic Valve Implantation) Registry. *Journal of the American College of Cardiology* 2011;58:2130-8.

10. Sinning JM, Vasa-Nicotera M, Chin D et al. Evaluation and management of paravalvular aortic regurgitation after transcatheter aortic valve replacement. *Journal of the American College of Cardiology* 2013;62:11-20.
11. Khalique OK, Hahn RT, Gada H et al. Quantity and location of aortic valve complex calcification predicts severity and location of paravalvular regurgitation and frequency of post-dilation after balloon-expandable transcatheter aortic valve replacement. *JACC Cardiovascular interventions* 2014;7:885-94.
12. Azzalini L, Ghoshhajra BB, Elmariah S et al. The aortic valve calcium nodule score (AVCNS) independently predicts paravalvular regurgitation after transcatheter aortic valve replacement (TAVR). *Journal of cardiovascular computed tomography* 2014;8:131-40.
13. John D, Buellesfeld L, Yucel S et al. Correlation of Device landing zone calcification and acute procedural success in patients undergoing transcatheter aortic valve implantations with the self-expanding CoreValve prosthesis. *JACC Cardiovascular interventions* 2010;3:233-43.
14. Grube E, Schuler G, Buellesfeld L et al. Percutaneous aortic valve replacement for severe aortic stenosis in high-risk patients using the second- and current third-generation self-expanding CoreValve prosthesis: device success and 30-day clinical outcome. *Journal of the American College of Cardiology* 2007;50:69-76.
15. Sellers RD, Levy MJ, Amplatz K, Lillehei CW. Left Retrograde Cardioangiography in Acquired Cardiac Disease: Technique, Indications and Interpretations in 700 Cases. *The American journal of cardiology* 1964;14:437-47.
16. Zoghbi WA, Chambers JB, Dumesnil JG et al. Recommendations for evaluation of prosthetic valves with echocardiography and doppler ultrasound: a report From the American Society of Echocardiography's Guidelines and Standards Committee and the Task Force on Prosthetic Valves, developed in conjunction with the American College of Cardiology Cardiovascular Imaging Committee, Cardiac Imaging Committee of the American Heart Association, the European Association of Echocardiography, a registered branch of the European Society of Cardiology, the Japanese Society of Echocardiography and the Canadian Society of

- Echocardiography, endorsed by the American College of Cardiology Foundation, American Heart Association, European Association of Echocardiography, a registered branch of the European Society of Cardiology, the Japanese Society of Echocardiography, and Canadian Society of Echocardiography. *J Am Soc Echocardiogr* 2009;22:975-1014; quiz 1082-4.
17. Kappetein AP, Head SJ, Genereux P et al. Updated standardized endpoint definitions for transcatheter aortic valve implantation: the Valve Academic Research Consortium-2 consensus document. *Journal of the American College of Cardiology* 2012;60:1438-54.
 18. Glodny B, Helmelt B, Trieb T et al. A method for calcium quantification by means of CT coronary angiography using 64-multidetector CT: very high correlation with Agatston and volume scores. *European radiology* 2009;19:1661-8.
 19. King G, Zeng L. Logistic regression in rare events data. *Political analysis* 2001;9:137-163.
 20. Athappan G, Patvardhan E, Tuzcu EM et al. Incidence, predictors, and outcomes of aortic regurgitation after transcatheter aortic valve replacement: meta-analysis and systematic review of literature. *Journal of the American College of Cardiology* 2013;61:1585-95.
 21. Ewe SH, Ng AC, Schuijff JD et al. Location and severity of aortic valve calcium and implications for aortic regurgitation after transcatheter aortic valve implantation. *The American journal of cardiology* 2011;108:1470-7.
 22. Leber AW, Kasel M, Ischinger T et al. Aortic valve calcium score as a predictor for outcome after TAVI using the CoreValve revalving system. *International journal of cardiology* 2013;166:652-7.
 23. Kasel AM, Cassese S, Bleiziffer S et al. Standardized imaging for aortic annular sizing: implications for transcatheter valve selection. *JACC Cardiovasc Imaging* 2013;6:249-62.
 24. Barbanti M, Leipsic J, Binder R et al. Underexpansion and ad hoc post-dilation in selected patients undergoing balloon-expandable transcatheter aortic valve replacement. *Journal of the American College of Cardiology* 2014;63:976-81.
 25. Yang TH, Webb JG, Blanke P et al. Incidence and severity of paravalvular aortic regurgitation with multidetector computed tomography nominal area oversizing or undersizing after

- transcatheter heart valve replacement with the Sapien 3: a comparison with the Sapien XT. *JACC Cardiovascular interventions* 2015;8:462-71.
26. Nombela-Franco L, Rodes-Cabau J, DeLarochelliere R et al. Predictive factors, efficacy, and safety of balloon post-dilation after transcatheter aortic valve implantation with a balloon-expandable valve. *JACC Cardiovascular interventions* 2012;5:499-512.
 27. Takagi K, Latib A, Al-Lamee R et al. Predictors of moderate-to-severe paravalvular aortic regurgitation immediately after CoreValve implantation and the impact of postdilatation. *Catheterization and cardiovascular interventions : official journal of the Society for Cardiac Angiography & Interventions* 2011;78:432-43.
 28. Barbanti M, Petronio AS, Capodanno D et al. Impact of balloon post-dilation on clinical outcomes after transcatheter aortic valve replacement with the self-expanding CoreValve prosthesis. *JACC Cardiovascular interventions* 2014;7:1014-21.
 29. Taramasso M, Pozzoli A, Latib A et al. New devices for TAVI: technologies and initial clinical experiences. *Nat Rev Cardiol* 2014;11:157-67.

국문 초록

목표: 본 연구에서는 경피적 대동맥판막 치환술을 시행 받은 환자들을 대상으로 대동맥판막 석회화의 비대칭 정도를 분석하고, 이러한 지표가 시술 후 판막주위 역류 발생 위험 및 추가 풍선확장의 성적을 예측할 수 있는지를 평가하고자 하였다.

배경: 대동맥판막 석회화의 비대칭 정도가 경피적 대동맥판막 치환술 후 판막주위 역류 발생 위험과 추가 풍선확장의 성적에 미치는 영향에 대해서는 연구된 바가 없다.

방법: 중증의 대동맥판막 협착증이 진단되어 자가팽창성 인공판막으로 경피적 대동맥판막 치환술을 시행 받은 85명의 환자들을 모집하여 연구를 시행하였다. 전산화 단층촬영 혈관조영술 영상을 분석하여 대동맥판막의 총 석회화 정도와 석회화 비대칭 정도를 정량화하였다. 대동맥판막 엽을 기준으로 한 구분에 한정되지 않게 여러 2분면을 생성하여 각각의 2분면에 해당하는 석회화 용적 점수의 차이를 계산하고, 이 중에서 가장 큰 수치를 대동맥판막 석회화 비대칭 지표로 정의하였다. 환자 판막륜의 크기에 대한 인공판막의 상대적인 크기를 고려하기 위하여 둘레 크기 저평가 지표를 계산하여 분석에 이용하였다. 시술 후 불완전한 밀폐로 인해 인공판막과 판막륜 사이의 공간으로 비정상적인 혈류가 관찰되는 경우에 판막주위 역류가 발생하였다고 정의하였다. 본 연구의 일차 종결점은 시술 후 발생한 유의한 판막주위 역류이며, 이는 중등도 이상의 판막주위 역류로 정의하였다. 인공판막 저팽창에 의해 발생한 판막주위 역류를 호전시킬 수 있는 술기인 추가 풍선확장에 대한 치료 성적을 이차 종결점으로 설정하였다.

결과: 대동맥판막 석회화의 총량과 비대칭 지표는 모두 중등도 이상 판막주위 역류의 발생 위험을 유의하게 예측하였으며, 대동맥판막 석회화 비대칭 지표가 석회화 총량보다 우수한 예측력을 보였다 (area under the curve = 0.863 versus 0.760, p for difference = 0.006). 둘레 크기 저평가 지표를 포함하여 다변량 분석을 시행하였을 때, 대동맥판막 석회화

비대칭 지표는 중등도 이상 관막주위 역류 발생의 독립적이고 유의한 예측인자였다. 대동맥판막의 전체적인 석회화 정도가 심하더라도 (대동맥판막 석회화 총량 $>1099.1 \text{ mm}^3$) 석회화의 분포가 대칭적인 환자의 경우에는 (대동맥판막 석회화 비대칭 지표 $\leq 272.8 \text{ mm}^3$) 중등도 이상의 관막주위 역류가 발생하지 않았다. 추가 풍선확장에 대한 치료 성적을 종결점으로 동일한 분석을 시행하였을 때, 대동맥판막 석회화 비대칭 지표만이 이를 유의하게 예측할 수 있는 유일한 인자였다 (area under the curve = 0.775, $p = 0.004$). 둘레 크기 저평가 지표에 대동맥판막 석회화 비대칭 지표를 추가하였을 때, 예측 모형의 분별 능력이 유의하게 증가되고 위험도 추정의 분류 정도 또한 유의하게 향상되었으나, 대동맥판막 석회화 총량의 경우에는 이러한 추가적인 예후적 가치가 관찰되지 않았다.

결론: 전산화 단층촬영 혈관조영술을 활용한 대동맥판막 석회화의 비대칭 정도에 대한 평가는, 자가팽창성 인공판막으로 경피적 대동맥판막 치환술을 시행 받는 환자들에서 시술 후 유의한 관막주위 역류의 발생 위험과 추가 풍선확장의 치료 성적에 대한 유용한 예측 정보를 제공한다.

주요어: 비대칭적 대동맥판막 석회화, 경피적 대동맥판막 치환술, 관막주위 역류, 추가 풍선확장, 전산화 단층촬영 혈관조영술

학번: 2013-30834